Lone-Pair Distribution and Plumbite Network Formation in High Lead Silicate Glass, 80PbO.20SiO$_2$

Oliver L. G. Alderman, Alex C. Hannon, Diane Holland, Steve Feller, Gloria Lehr, Adam J. Vitale, Uwe Hoppe, Martin von Zimmerman, Anke Watenphul

Supplementary Information

S1. Full experimental details

X-ray Diffraction

Wiggler beamline BW5[59] on the DORIS III synchrotron, HASYLAB at DESY, was used for an x-ray diffraction measurement of the powdered tetralead silicate glass which was held inside a 1.5 mm diameter silica glass capillary (20 µm wall thickness). Measurements of an empty capillary and the empty instrument were made to allow removal of background scattering. The white beam, which has a polarisation factor of 0.92, was monochromated with a SiGe-gradient crystal to an energy of 84.768 keV (wavelength 0.14626 Å), calibrated by measurement of a lanthanum hexaboride standard. The beam profile was 2 x 2 mm, chosen to be larger than the sample diameter. The choice of x-ray energy is optimised so as to minimise the photoelectric absorption cross-section whilst avoiding fluorescence associated with the Pb K-edge at 88.0 keV. Use of such high energy x-rays also makes accessible a large $Q_{max} = 23.62$ Å^{-1} at the maximum scattering angle of the detector arm which is 32.0^o. The corresponding minimum scattering angle was 0.5^o ($Q_{min} = 0.38$ Å^{-1}). The data were collected in three angular ranges using different in-beam attenuators. These ranges were $0.5 \leq 2\theta \leq 8^o$, $7 \leq 2\theta \leq 17^o$ and $16 \leq 2\theta \leq 32^o$ (no in-beam attenuation), with a step size of 0.05^o. This was to ensure that the count rate in the Ge detector did not greatly exceed 5×10^4 counts per second. All sets of data were combined after omission of bad points, dead-time correction ($\tau = 2.3$ µs), normalisation to the incident beam monitor counts, correction for the geometrical arrangement of the detector and sample and scaling as required for datasets for which different levels of in-beam attenuation was used. At this point the program GudrunX[69,70] was used to correct the data for the effects of polarisation, absorption and multiple scattering, removal of backgrounds, normalisation using the Krogh-Moe and Norman method, and extraction of $i^X(Q)$ by removal of the self-scattering (including the Compton fraction) and sharpening. A sample of commercial amorphous silica was measured in an identical manner and the results are presented below (Figs. S1 and S2).

Neutron Diffraction

A time-of flight neutron diffraction measurement was made using the GEM[61] diffractometer at the ISIS Facility, Rutherford Appleton Laboratory, UK. This instrument has a large number of detectors which cover a large solid angle, and therefore offers high count rates over a large portion of reciprocal space. The glass, in the form of small (few mm^2) flakes, as obtained from the twin-roller-quenching process, was loaded into a thin (25 μm) walled vanadium can of internal diameter 8.3 mm and this was held inside the evacuated sample tank through which the incident neutron beam passed. The beam cross section was 40 x 40 mm, larger than the diameter, but shorter than the 60 mm height of the cylindrical sample. Data were acquired for 1000 μAhr of proton beam current, corresponding to approximately 6 to 7 hours of counting time. This yielded sufficient statistics to justify use of a maximum scattering vector of $Q_{max} = 40.0$ Å^{-1} for the Fourier transform. Measurements were also performed on an empty vanadium can, the empty instrument, and an 8 mm vanadium rod for normalisation purposes and to allow for subtraction of background signals. Corrections for absorption, multiple scattering, inelasticity effects, backgrounds, normalisation and reduction of the measured data to obtain $i^N(Q)$ were performed using the GudrunN[70] software and the Atlas[74] suite of programs. A quadratic fit to the data below $Q = 0.7$ Å^{-1} was used to extrapolate back to $Q = 0$. An 8 mm diameter silica glass rod was measured in an identical manner (without the need for a V can), and the results are presented below (Figs. S1 and S3).

EDX measurements

Glass composition was measured using energy dispersive x-ray spectroscopy (EDX) in a Zeiss SUPRA 55-VP field emission gun scanning electron microscope (FEGSEM) operating at an accelerating voltage of 20 kV. Samples were mounted on aluminium stubs using an organic silver paste and carbon coated using a vacuum evaporator to provide a conduction pathway and avoid surface charging of the glass. EDX spectra were collected over 100 s exposure times at various points on the surface of a number of different glass flakes. Quantification of the glass composition was based on the integrated intensities of the Si K and Pb L lines of the spectra after background subtraction and correction for Z dependent electron backscatter and stopping power, absorption and fluorescence, collectively known as ZAF correction, using the EDAX Genesis software which employs internal standards.

There is a claim in the literature of a 96 mol% PbO lead silicate glass,[82] and we made a glass by closely following the preparation method described in this report. However, EDX measurements revealed a glass composition of $(72.8 \pm 1.0)PbO.(16.6 \pm 0.5)SiO_2.(10.6 \pm 0.5)Al_2O_3$, indicating a large contamination from the crucible, which had approximate composition $84SiO_2.16Al_2O_3$ (but also contained small amounts of Ca, Mg, Na, P and K).

S2. Total Scattering Formalism

The quantity measured in a total scattering experiment is the differential scattering cross-section,

$$\frac{d\sigma}{d\Omega} = I^S(Q) + i(Q)$$

(S1)

of a given radiation type from a given target as a function of the scattering vector $\mathbf{Q}$, where only its magnitude, $Q = (4\pi/\lambda)\sin\theta$, need be considered for an isotropic sample. The differential cross-section, eqn (S1), can be split into a self-scattering term, $I^S(Q)$, and a distinct scattering term, $i(Q)$, the latter of which contains the information pertaining to the atomic arrangement of the constituent atoms of the sample. The self-scattering, $I^S(Q)$, can be calculated given the composition of the sample and the scattering lengths or form factors for the constituent atoms, and in general includes an inelasticity correction term which can be calculated only approximately in the case of both neutrons and x-rays. Hence the distinct scattering term can be obtained from the measured differential scattering cross-section. $i(Q)$ can be written as a weighted sum over the partial pair structure factors $S_{ij}(Q)$ relating to distinct scattering between specific atom pairs where i and j denote elemental species:

$$i(Q) = \sum_{i,j=1}^{n} c_i c_j f_i(Q) f_j(Q)(S_{ij}(Q) - 1)$$

(S2)

In eqn (S2), n is the number of elements present in the sample, c_i are the atomic fractions and $f_i(Q)$ denotes either x-ray form factor, or Q-independent bound coherent neutron scattering length, $\bar{b}_i$. In the x-ray case a modified function

$$i^X(Q) = \frac{i(Q)}{\left(\sum_{i=1}^{n} c_i f_i(Q)\right)^2}$$

(S3)

is defined in which the denominator is used as an approximate means of dividing out, or "sharpening",[96] the form factor dependence of $i(Q)$. It is convenient to define neutron (N) and x-ray (X) weighting factors as follows:

$$w_{ij}^N(Q) = c_i c_j \bar{b}_i \bar{b}_j$$

(S4)

$$w_{ij}^X(Q) = \frac{c_i c_j f_i(Q) f_j(Q)}{\left(\sum_{i=1}^{n} c_i f_i(Q)\right)^2}$$

(S5)

The weighting factors appropriate to the glass composition used in the present study are shown in Fig. 1, where the $\bar{b}_i$ are taken from Sears[97] and the free atom x-ray $f_i(Q)$ from Waasmaier and Kirfel.[98] The factor $(2 - \delta_{ij})$, with δ_{ij} the Kronecker delta, has been included in Fig. 1 such that the values plotted are appropriate to the $n(n+1)/2 = 6$ unique partial structure factors, rather than the total $n^2 = 9$ terms.

The real-space total correlation functions, which are functions of the interatomic distance, r, for the two radiation types are defined as follows:

$$T^R(r) = T^{R,0}(r) + \frac{2}{\pi}\int_0^\infty Qi^R(Q)M(Q)\sin(rQ)\,\mathrm{d}Q \qquad (S6)$$

where $R = N$ or X denotes the radiation type (and $i^N(Q)$ is obtained simply by subtraction of the self-scattering from the total scattering, see eqn (S1), whilst $i^X(Q)$ is defined according to eqn (S3)), and $M(Q)$ is a modification function which can be chosen to reduce the effects of the finite limits $(0 < Q \leq Q_{max})$ of the integral which are used in practice. In this study the $M(Q)$ due to Lorch[75] is chosen. The $T^{R,0}(r)$ represent average scattering density terms and are given by:

$$T^{N,0}(r) = 4\pi\rho_0 r\left(\sum_{i=1}^n c_i \bar{b}_i\right)^2 \qquad (S7)$$

$$T^{X,0}(r) = 4\pi\rho_0 r \qquad (S8)$$

with ρ_0 the atomic number density. In analogy to eqn (S2), the total correlation functions can be written as sums of terms corresponding to individual atom pairs:

$$T^R(r) = \sum_{i,j=1}^n \frac{1}{c_j} t_{ij}(r) \otimes k_{ij}^R(r) \qquad (S9)$$

where $\otimes$ denotes the convolution operation and

$$k_{ij}^R(r) = \frac{1}{\pi}\int_0^\infty w_{ij}^R(Q)\cos Qr\,\mathrm{d}Q \qquad (S10)$$

are the Fourier transforms of the weighting functions in eqns (S4) and (S5). The partial pair correlation functions $t_{ij}(r)$ are related to the commonly used pair correlation functions $g_{ij}(r)$ by

$$t_{ij}(r) = 4\pi\rho_j r g_{ij}(r) \qquad (S11)$$

where $\rho_j = c_j\rho_0$ and the $g_{ij}(r)$ are defined as

$$g_{ij}(r) = \frac{n_{ij}(r)}{4\pi\rho_j r^2\,\mathrm{d}r} . \qquad (S12)$$

Finally the functions $n_{ij}(r)$ are simply defined as the average number of atoms of element j inside a distance interval $(r, r + dr)$ from an atom of element i, see, for example, Keen[99] for a disambiguation of the various functions defined in the literature.

A single interatomic separation, r_{ij}, with root mean square (RMS) deviation $<u_{ij}^2>^{1/2}$, gives rise to a distinct scattering signal

$$i_{ij}^R(Q) = N_{ij}w_{ij}^R(Q)\frac{\sin(Qr_{ij})}{c_iQr_{ij}}\exp\left(\frac{-\left\langle u_{ij}^2\right\rangle Q^2}{2}\right), \qquad (S13)$$

and the area, A_{ij}^{R}, of the corresponding (symmetric) real-space peak, relates to the average coordination number

$$N_{ij} = \frac{r_{ij} A_{ij}^{R} c_j \int_0^{Q_{max}} dQ}{(2 - \delta_{ij}) \int_0^{Q_{max}} w_{ij}^{R}(Q) dQ} = \frac{c_j}{c_i} N_{ji} \quad .$$

(S14)

A general definition of the coordination number, which does not pertain to a symmetric real-space peak, can be written as

$$N'_{ij}(r_1, r_2) = \int_{r_1}^{r_2} r t_{ij}(r) dr = \frac{c_j}{c_i} N'_{ji}(r_1, r_2) \quad .$$

(S15)

S3. Neutron and X-ray diffraction from a vitreous SiO$_2$ standard

The functions $i^X(Q)$ and $i^N(Q)$ measured for vitreous silica are shown in Fig. S1. Their Fourier transforms, $T^X(r)$ and $T^N(r)$, are shown in Figs. S2 and S3 respectively. The Si-O and O-O peaks shown in Figs. S2 and S3 were derived by fitting to the neutron $T^N(r)$, whilst the Si-Si peak was derived by fitting to the x-ray $T^X(r)$, holding the peak parameters for the Si-O and O-O peaks fixed. Peak parameters are given in Table S1. It is clear from this analysis that both x-ray and neutron diffraction yield quantitatively accurate coordination numbers. The Si-Si coordination is overestimated due to overlap in this region with Si-2nd O and O-2nd O[59] which was not accounted for in the fitting procedure. The Si-O and O-O coordination numbers are damped below their expected values of 4 and 6 as a result of the Q-space resolution of the measurements. This was taken into account when predicting the area of the O-O correlation for the 80PbO.20SiO$_2$ glass.
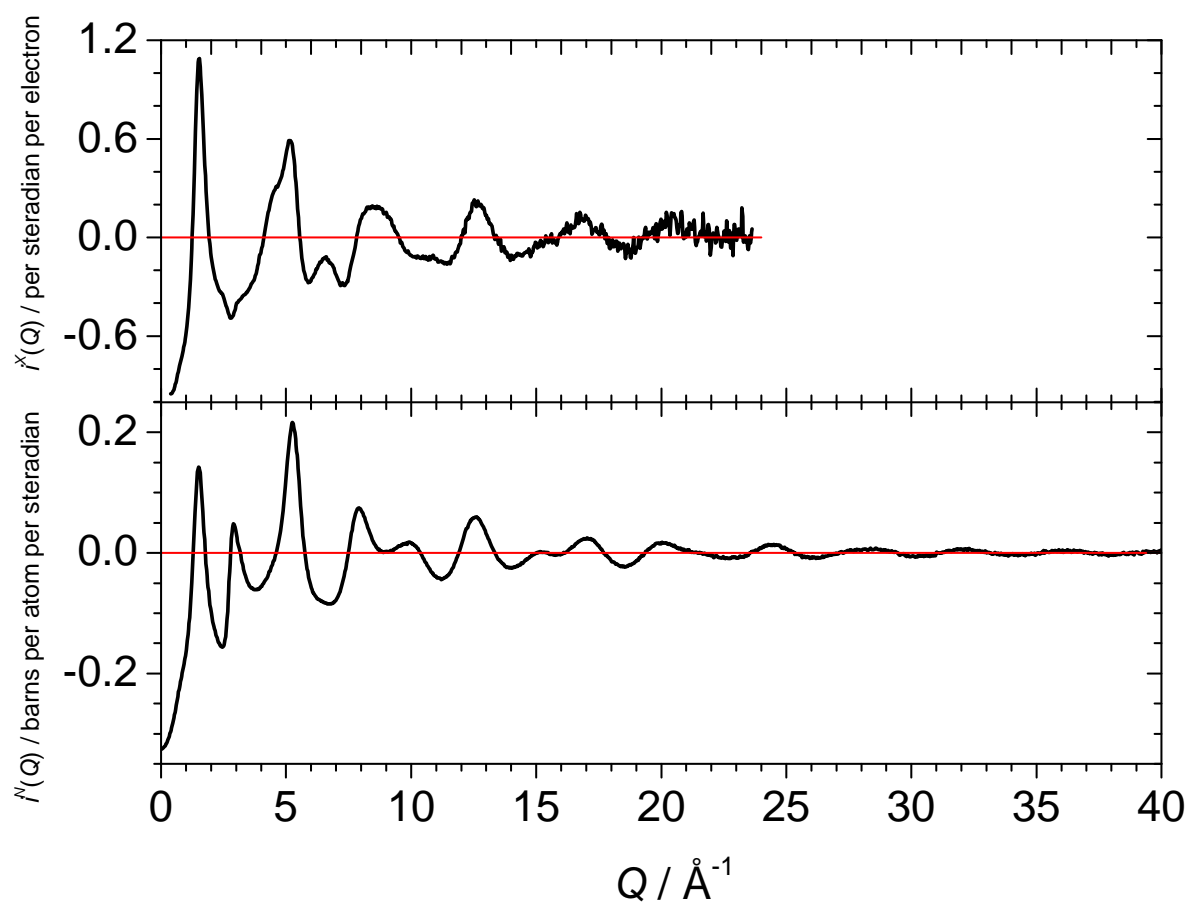

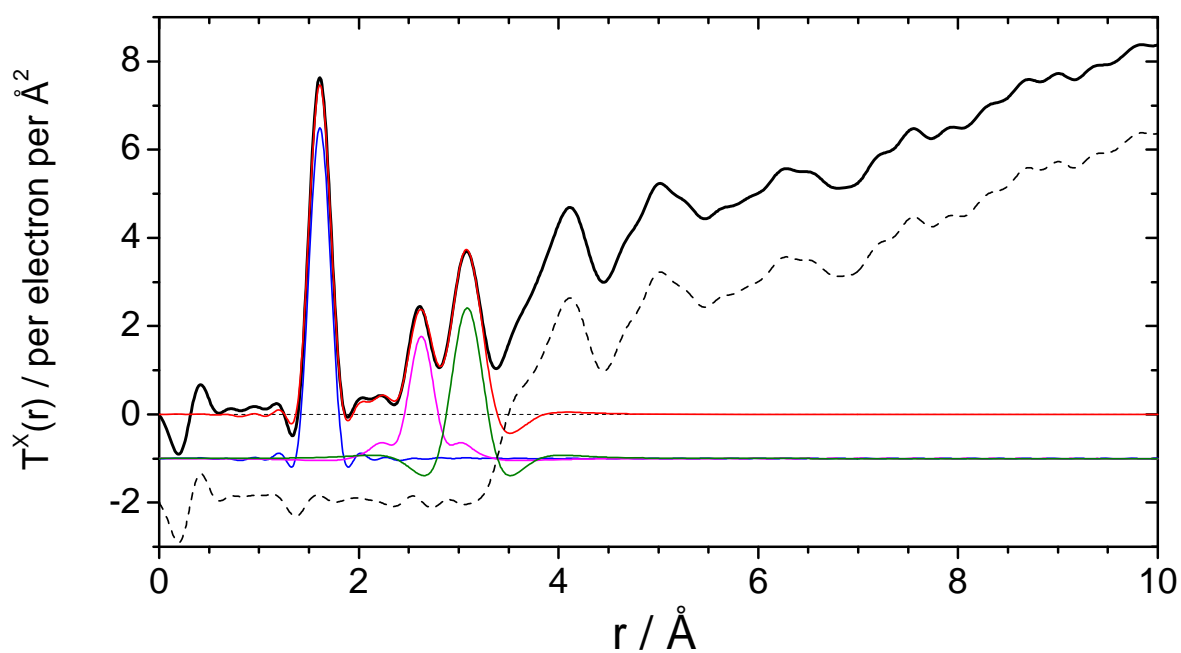Figure S1: The functions $i^X(Q)$ and $i^N(Q)$ measured for pure vitreous SiO$_2$.

Figure S2: $T^X(r)$ (thick black line), the Fourier transform of the function $i^X(Q)$ shown in Fig. S1. The summed peak fits are overlaid (thin red line), and individual peaks vertically offset below. Si-O: blue line, O-O: magenta line, Si-Si: green line. The residual is shown as a dashed black line, further offset for clarity.
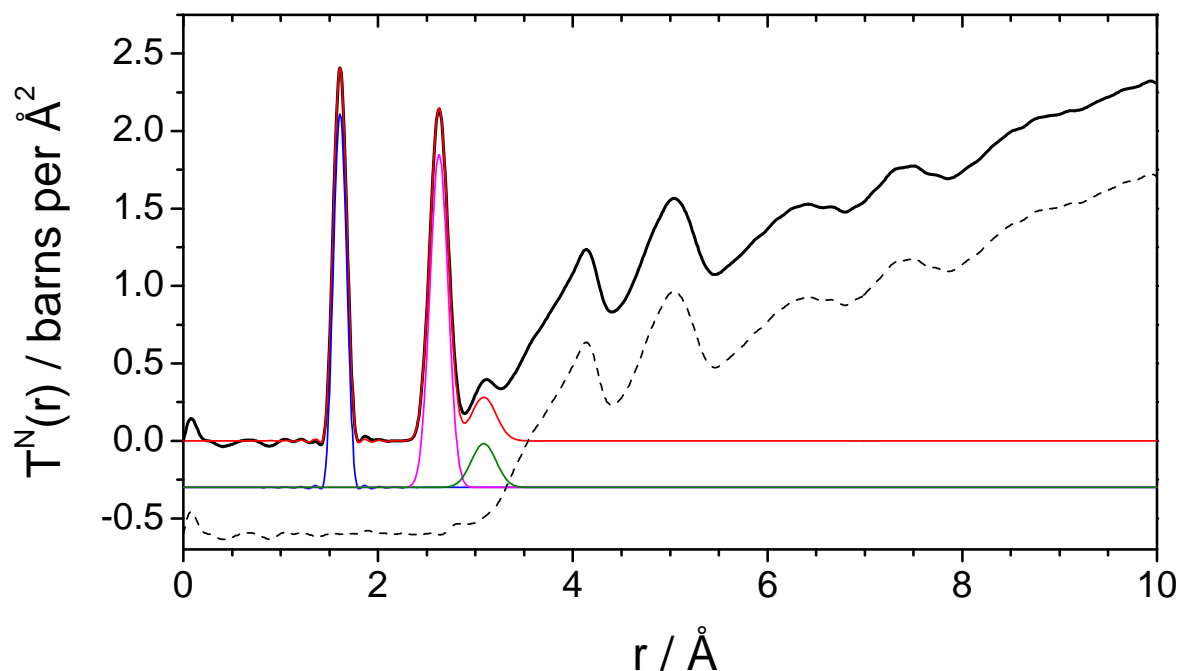

Figure S3: $T^N(r)$ (thick black line), the Fourier transform of the function $i^N(Q)$ shown in Fig. S1. The summed peak fits are overlaid (thin red line), and individual peaks vertically offset below. Si-O: blue line, O-O: magenta line, Si-Si: green line. The residual is shown as a dashed black line, further offset for clarity.

Table S1: Parameters from peak fitting to $T^N(r)$ and $T^X(r)$ measured for silica glass. Statistical errors from the fitting procedure are given in parentheses.

Atom pair i-j	r_{ij}, Å	$\langle u_{ij}^2 \rangle^{1/2}$, Å	N_{ij}
Si-O	1.6093(3)	0.0419(5)	3.96(2)
O-Si			1.98(1)
O-O [SiO_4]	2.6257(8)	0.0786(9)	5.79(4)
Si-Si*	3.085(2)	0.118(3)	4.80(9)

*Approximate due to overlap[59] in this region with Si-2nd O and O-2nd O which was not accounted for in the fitting procedure.
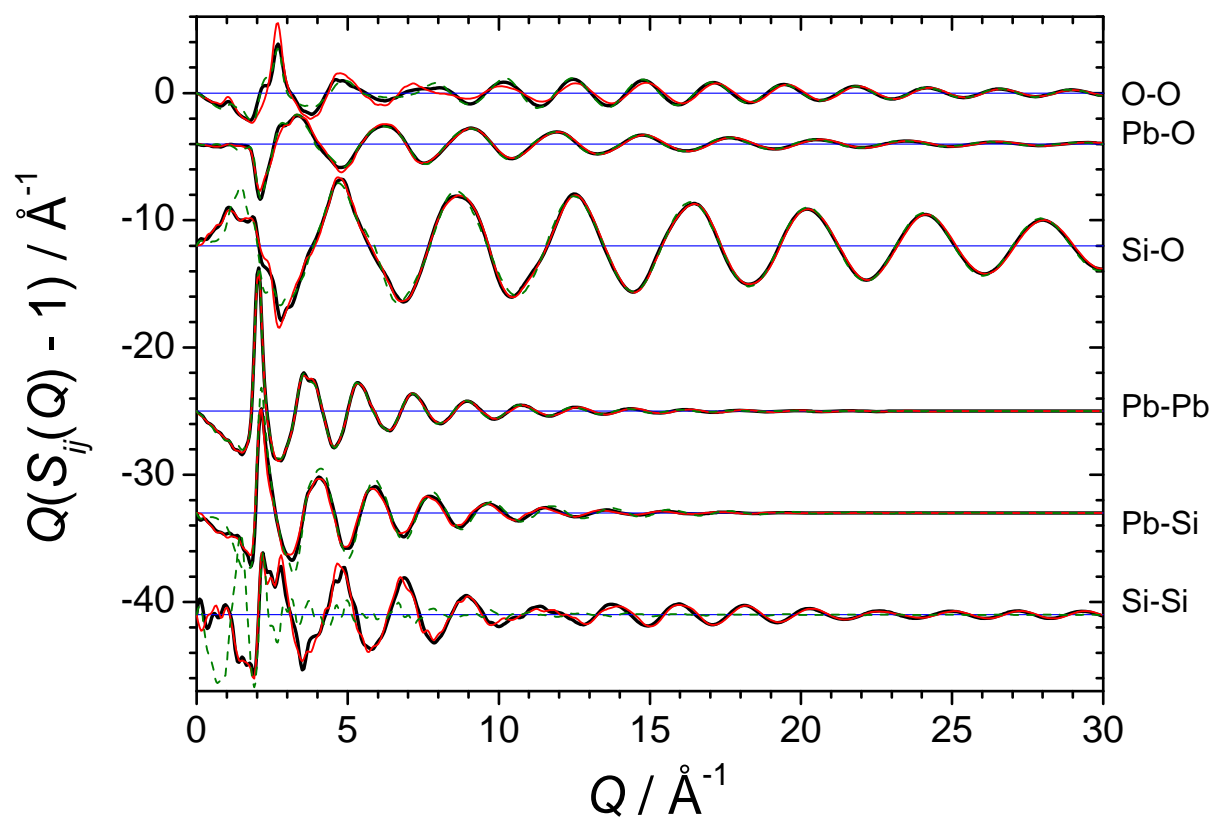
S4. Additional EPSR Modelling Results

Figure S4: Partial pair interference functions extracted from the EPSR models of the 80PbO.20SiO$_2$ glass. Ionic model: thick black lines, lone-pair model: thin red lines, Q^0 model: green dashed lines. Vertically offset for clarity.
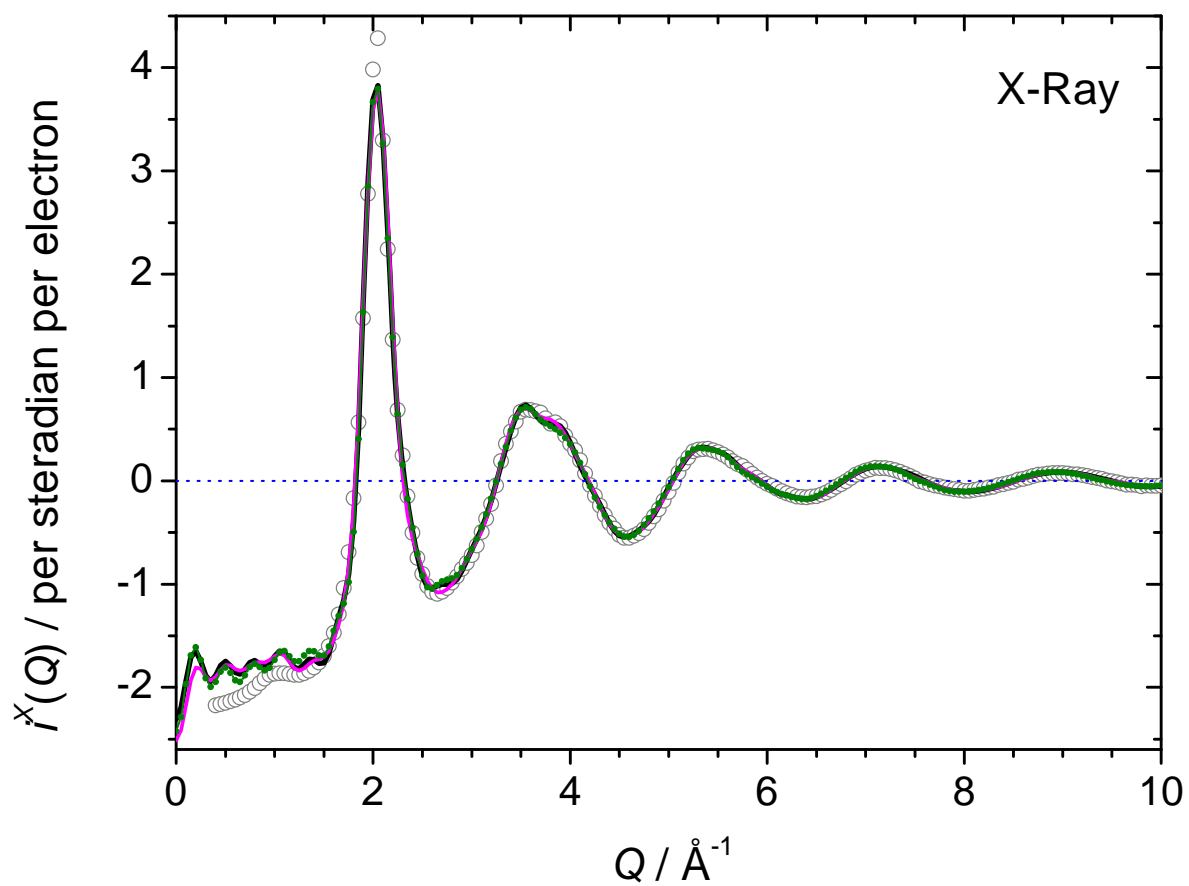
Figure S5: Distinct x-ray scattering function measured (open grey circles) and extracted from the EPSR models of the $80PbO.20SiO_2$ glass. Ionic model: thick black line, lone-pair model: thin magenta line, Q^0 model: green line with points.
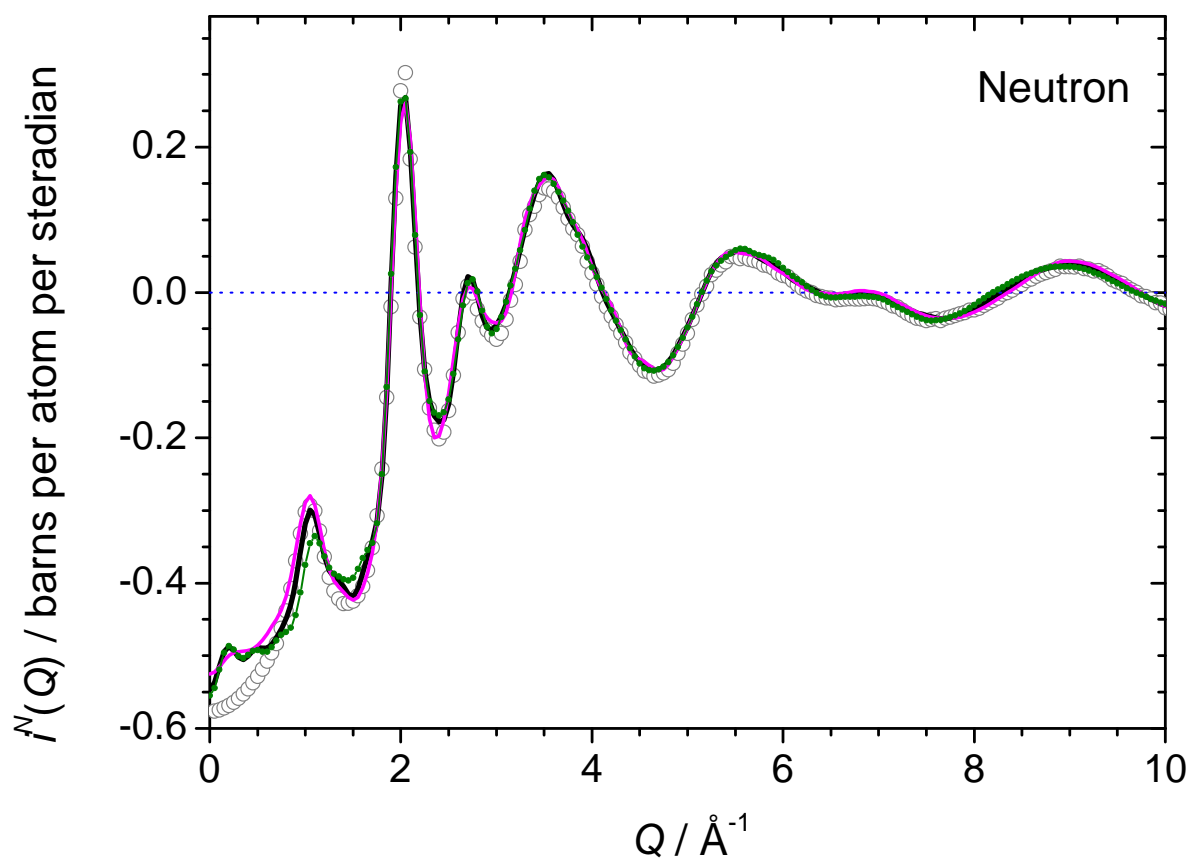
Figure S6: Distinct neutron scattering function measured (open grey circles) and extracted from the EPSR models of the 80PbO.20SiO$_2$ glass. Ionic model: thick black line, lone-pair model: thin magenta line, Q^0 model: green line with points.
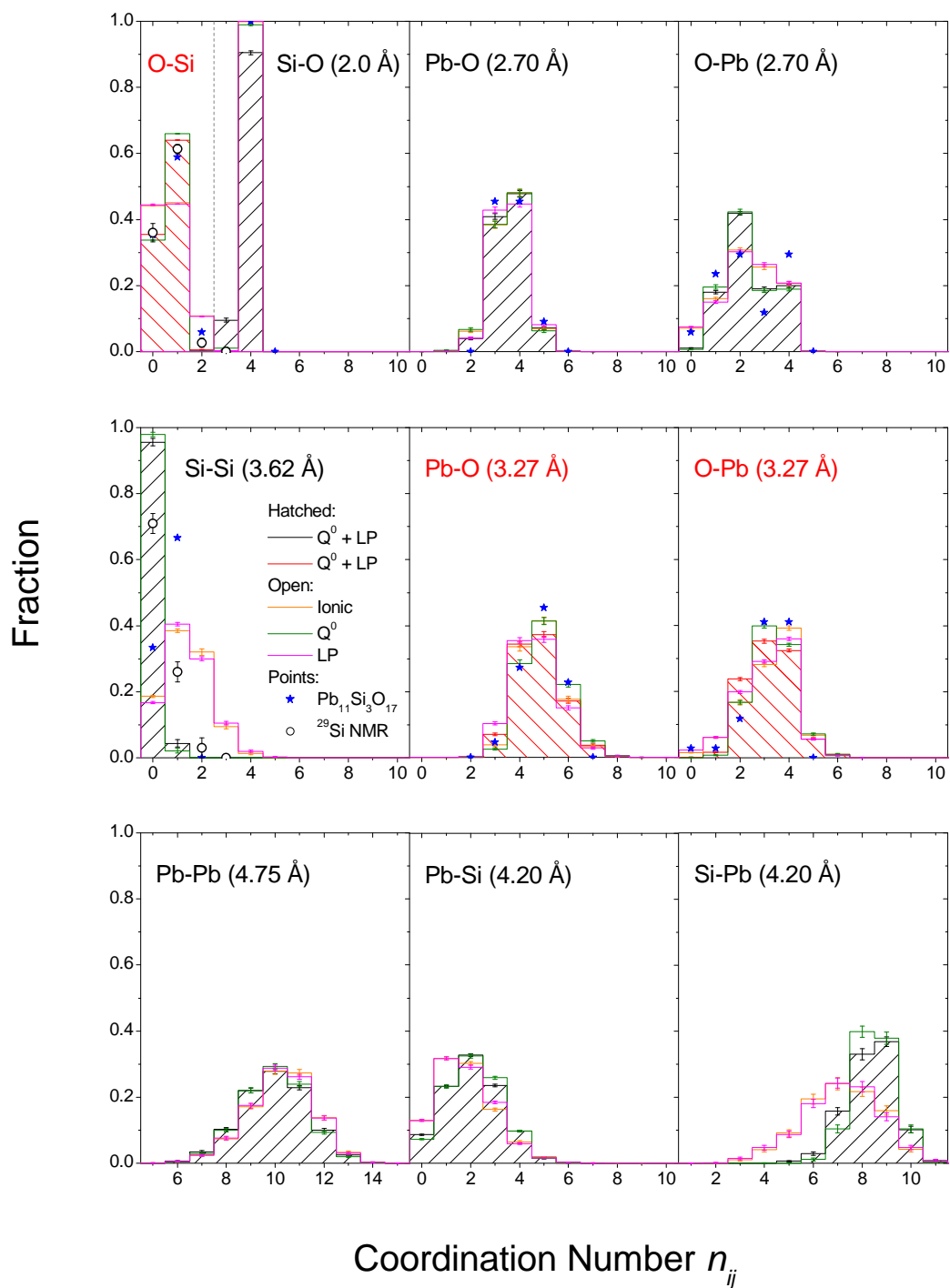
Figure S7: Coordination number distributions from the four EPSR models of the 80PbO.20SiO$_2$ glass, compared to those of Pb$_{11}$Si$_3$O$_{17}$[45] and the Si-Si and O-Si CNDs calculated from the Q species distribution measured by ^{29}Si MAS NMR.[23] Upper cut-off radii are given in parentheses. Numerical values are tabulated in Table 5.

Table S2: Analysis of the [OSi$_p$Pb$_q$] bonding configurations of oxygen within crystalline Pb$_{11}$Si$_3$O$_{17}$.[45] Results for two different radial cutoffs, r_2 (shown in parentheses), are given.

Coordination Number	% (2.70 Å)	% (3.27 Å)	Species	p	q	% (2.70 Å)	% (3.27 Å)
2	35.14	2.70	OSi$_2$	2	0	8.11	2.70
			OPbSi	1	1	27.03	0
			OPb$_2$	0	2	0	0
3	32.43	18.92	OSi$_3$	3	0	0	0
			OPbSi$_2$	2	1	0	5.41
			OPb$_2$Si	1	2	27.03	13.51
			OPb$_3$	0	3	5.41	0
4	32.43	72.97	OSi$_4$	4	0	0	0
			OPbSi$_3$	3	1	0	0
			OPb$_2$Si$_2$	2	2	0	0
			OPb$_3$Si	1	3	5.41	40.54
			OPb$_4$	0	4	27.03	32.43
5	0	5.41	OPb$_4$Si	1	4	0	5.41
Average N'_{OX}	2.97	3.81				2.97	3.81

S5. Linking the silicate Q^n speciation to the fraction of plumbite oxygen

Consider three types of oxygen: bridging (B), non-bridging (NB) and plumbite (P), all of which are defined by their O-Si coordination numbers of 2, 1 and 0 respectively. The sum of their fractions is

$$f_B + f_{NB} + f_P = 1$$

(S16)

and the average O-Si coordination number is

$$N_{OSi} = f_{NB} + 2f_B = N_{SiO}\frac{(1-x)}{(2-x)}$$

(S17)

where x is the mole fraction of MO in a composition of xMO.(1-x)SiO$_2$. The Q^n speciation, with n the number of bridging oxygen about a four coordinated silicon, can be related directly to the ratio

$$\frac{f_B}{f_B + f_{NB}} = \frac{\sum_{n=0}^{4}\frac{n}{2}Q^n}{\sum_{n=0}^{4}\left(4-\frac{n}{2}\right)Q^n}$$

(S18)

where the Q^n represent fractions of Q^n species. Now since $N_{SiO} = 4$ implicitly, the three unknown quantities f_B, f_{NB} and f_P can all be calculated given the Q^n speciation, which can be estimated from the ^{29}Si MAS NMR spectrum.
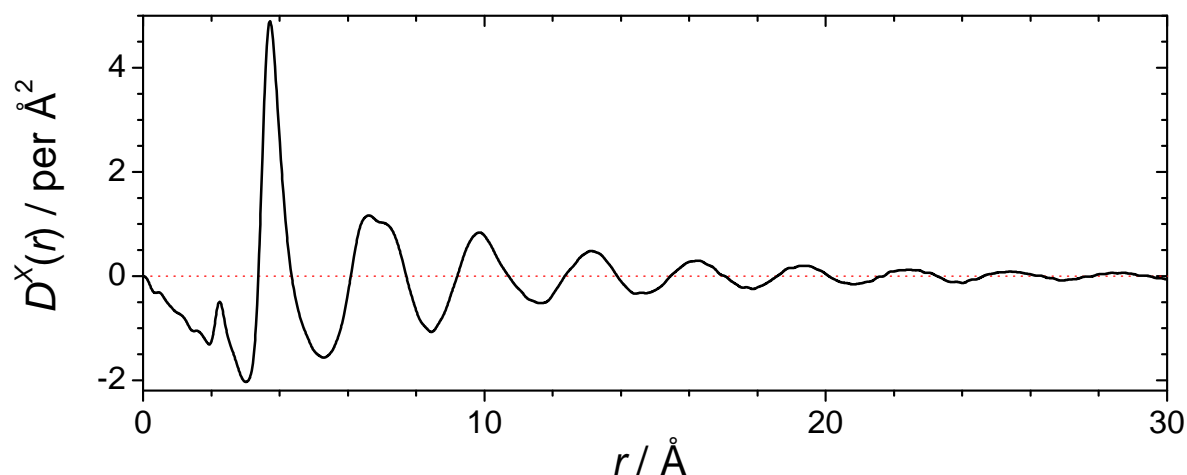
Figure S8: X-ray differential correlation function for $80PbO.20SiO_2$ glass shown out to 30 Å in order to show the extent of the real-space oscillations arising from the Pb-Pb term.

References

1   W. H. Dumbaugh and J. C. Lapp, *J. Am. Ceram. Soc.*, 1992, **75**, 2315-2326.

2   S. R. Friberg and P. W. Smith, *IEEE J. Quantum Elect.*, 1987, **23**, 2089-2094.

3   E. R. Barney, A. C. Hannon, N. Laorodphan and D. Holland, *J. Phys. Chem. C*, 2011, **115**, 14997-15007.

4   M. Imaoka and A. Hasegawa, *J. Ceram. Assoc. Jap.*, 1980, **88**, 141-150.

5   H. Morikawa, Y. Takagi and H. Ohno, *J. Non-Cryst. Solids*, 1982, **53**, 173-182.

6   H. Ohno, K. Igarashi, Y. Takagi, H. Toratani, K. Furukawa, J. Mochinaga, T. Nakamura and T. Izumitani, *J. Jpn. Inst. Met.*, 1983, **47**, 132-141.

7   H. Hasegawa and M. Imaoka, *J. Non-Cryst. Solids*, 1984, **68**, 157-158.

8   H. Morikawa, Y. Takagi and H. Ohno, *J. Non-Cryst. Solids*, 1984, **68**, 159-162.

9   M. Imaoka, H. Hasegawa and I. Yasui, *J. Non-Cryst. Solids*, 1986, **85**, 393-412.

10   K. Yamada, A. Matsumoto, N. Niimura, T. Fukunaga, N. Hayashi and N. Watanabe, *J. Phys. Soc. Jpn.*, 1986, **55**, 831-837.

11   K. Suzuya, D. L. Price, M. L. Saboungi and H. Ohno, *Nucl. Instrum. Meth. B*, 1997, **133**, 57-61.

12   K. Suzuya, S. Kohara and H. Ohno, *Jpn. J. Appl. Phys. Part 1*, 1999, **38**, 144-147.

13   U. Hoppe, R. Kranold, A. Ghosh, C. Landron, J. Neuefeind and P. Jovari, *J. Non-Cryst. Solids*, 2003, **328**, 146-156.

14   T. Takaishi, M. Takahashi, J. Jin, T. Uchino, T. Yoko and M. Takahashi, *J. Am. Ceram. Soc.*, 2005, **88**, 1591-1596.

15   S. Kohara, H. Ohno, M. Takata, T. Usuki, H. Morita, K. Suzuya, J. Akola and L. Pusztai, *Phys. Rev. B*, 2010, **82**, 134209 134201-134207.

16   F. Fayon, C. Landron, K. Sakurai, C. Bessada and D. Massiot, *J. Non-Cryst. Solids*, 1999, **243**, 39-44.

17   V. R. Mastelaro, E. D. Zanotto, N. C. Lequeux and R. Cortes, *J. Non-Cryst. Solids*, 2000, **262**, 191-199.

18   J. Rybicki, A. Rybicka, A. Witkowska, G. Bergmanski, A. Di Cicco, M. Minicucci and G. Mancini, *J. Phys.: Condens. Mat.*, 2001, **13**, 9781-9797.

19   H. Hosono, H. Kawazoe and T. Kanazawa, *J. Ceram. Assoc. Jap.*, 1982, **90**, 544-551.

20   E. Lippmaa, A. Samoson, M. Magi, R. Teeaar, J. Schraml and J. Gotz, *J. Non-Cryst. Solids*, 1982, **50**, 215-218.

21   R. Dupree, N. Ford and D. Holland, *Phys. Chem. Glasses*, 1987, **28**, 78-84.

22   F. Fayon, C. Bessada, D. Massiot, I. Farnan and J. P. Coutures, *J. Non-Cryst. Solids*, 1998, **232**, 403-408.

23   S. Feller, G. Lodden, A. Riley, T. Edwards, J. Croskrey, A. Schue, D. Liss, D. Stentz, S. Blair, M. Kelley, G. Smith, S. Singleton, M. Affatigato, D. Holland, M. E. Smith, E. I. Kamitsos, C. P. E. Varsamis and E. Ioannou, *J. Non-Cryst. Solids*, 2010, **356**, 304-313.

24   L. Leventhal and A. J. Bray, *Phys. Chem. Glasses*, 1965, **6**, 113-125.

25   T. Yoko, K. Tadanaga, F. Miyaji and S. Sakka, *J. Non-Cryst. Solids*, 1992, **150**, 192-196.

26   B. M. J. Smets and T. P. A. Lommen, *J. Non-Cryst. Solids*, 1982, **48**, 423-430.

27   P. W. Wang and L. P. Zhang, *J. Non-Cryst. Solids*, 1996, **194**, 129-134.

28   I. A. Gee, D. Holland and C. F. McConville, *Phys. Chem. Glasses*, 2001, **42**, 339-348.

29   K. N. Dalby, H. W. Nesbitt, V. P. Zakaznova-Herzog and P. L. King, *Geochim. Cosmochim. Ac.*, 2007, **71**, 4297-4313.

30   T. Furukawa, S. A. Brawer and W. B. White, *J. Mater. Sci.*, 1978, **13**, 268-282.

31   C. A. Worrell and T. Henshall, *J. Non-Cryst. Solids*, 1978, **29**, 283-299.

32   B. Piriou and H. Arashi, *High Temp. Sci.*, 1980, **13**, 299-313.

33   L. P. Liu, *Z. Phys. B*, 1993, **90**, 393-399.

34   D. D. Meneses, M. Malki and P. Echegut, *J. Non-Cryst. Solids*, 2006, **352**, 769-776.

35   K. V. Damodaran, B. G. Rao and K. J. Rao, *Phys. Chem. Glasses*, 1990, **31**, 212-216.

36   G. Cormier, T. Peres and J. A. Capobianco, *J. Non-Cryst. Solids*, 1996, **195**, 125-137.

37   J. Rybicki, W. Alda, A. Rybicka and S. Feliziani, *Comput. Phys. Commun.*, 1996, **97**, 191-194.

38   T. Peres, D. A. Litton, J. A. Capobianco and S. H. Garofalini, *J. Non-Cryst. Solids*, 1997, **221**, 34-46.

39   T. Peres, D. A. Litton, J. A. Capobianco and S. H. Garofalini, *Philos. Mag. B*, 1998, **77**, 389-396.

40   A. Rybicka, J. Rybicki, A. Witkowska, S. Feliziani and G. Mancini, *Comp. Meth. Sci. Tech.*, 1999, **5**, 67-74.

41   G. Bergmanski, M. Bialoskorski, M. Rychcik-Leyk, A. Witkowska, J. Rybicki, G. Mancini, S. Frigio and S. Feliziani, *Task Quarterly*, 2004, **8**, 393-412.

42   M. L. Boucher and D. R. Peacor, *Z. Krist.*, 1968, **126**, 98-111.

43   L. S. D. Glasser, R. A. Howie and R. M. Smart, *Acta Cryst. B*, 1981, **37**, 303-306.

44   K. Kato, *Acta Cryst. B*, 1980, **36**, 2539-2545.

45   K. Kato, *Acta Cryst. B*, 1982, **38**, 57-62.

46   S. V. Krivovichev and P. C. Burns, *Zapiski Vserossijskogo Mineralogicheskogo Obshchestva*, 2004, **133**, 70-76.

47   W. Petter, A. B. Harnik and U. Keppler, *Z. Krist.*, 1971, **133**, 445-458.

48   R. G. Dickinson and J. B. Friauf, *J. Am. Chem. Soc.*, 1924, **46**, 2457-2463.

49   R. J. Hill, *Acta Cryst. C*, 1985, **41**, 1281-1284.

50   K. Fajans and N. J. Kreidl, *J. Am. Ceram. Soc.*, 1948, **31**, 105-114.

51   K. H. Sun, *J. Am. Ceram. Soc.*, 1947, **30**, 277-281.

52   A. C. Wright, in *Experimental Techniques of Glass Science*, ed. C. J. Simmons and O. H. El-Bayoumi, American Ceramic Society, Westerville, 1993, pp. 205-314.

53   R. L. McGreevy, *J. Phys.: Condens. Mat.*, 2001, **13**, R877-R913.

54   R. L. McGreevy and P. Zetterström, *J. Non-Cryst. Solids*, 2001, **293-295**, 297-303.

55   A. K. Soper, *Phys. Rev. B*, 2005, **72**, 104204

56   A. J. Havel, S. A. Feller, M. Affatigato and M. Karns, *Glass Technol.: Eur. J. Glass Sci. Technol. A*, 2009, **50**, 227-229.

57   *SciGlass Professional 7.3*, ITC Inc., 2008.

58   O. V. Mazurin, M. V. Strel'tsina, T. P. Shvaiko-Shvaikovskaya and A. O. Mazurina, *Glass Phys. Chem.*, 2003, **29**, 555-570.

59   H. F. Poulsen, J. Neufeind, H. B. Neumann, J. R. Schneider and M. D. Zeidler, *J. Non-Cryst. Solids*, 1995, **188**, 63-74.

60   J. A. Bearden and A. F. Burr, *Rev. Mod. Phys.*, 1967, **39**, 125.

61   A. C. Hannon, *Nucl. Instrum. Meth. A*, 2005, **551**, 88-107.

62   A. K. Soper, *J. Phys.: Condens. Mat.*, 2010, **22**, 404210.

63   A. K. Soper, *J. Phys.: Condens. Mat.*, 2011, **23**, 365402.

64   C. Pirovano, M. S. Islam, R. N. Vannier, G. Nowogrocki and G. Mairesse, *Solid State Ionics*, 2001, **140**, 115-123.

65   D. Lebellac, J. M. Kiat and P. Garnier, *J. Solid State Chem.*, 1995, **114**, 459-468.

66   D. T. Bowron and S. Diaz-Moreno, *J. Phys. Chem. B*, 2009, **113**, 11858-11864.

67   A. K. Soper, *Chem. Phys.*, 2000, **258**, 121-137.

68   A. K. Soper, *Chem. Phys.*, 1996, **202**, 295-306.

69   A. K. Soper and E. R. Barney, *J. Appl. Cryst.*, 2011, **44**, 714-726.

70   A. K. Soper, *Rutherford Appleton Laboratory Technical Report, RAL-TR-2011-013*, 2011.

71   J. Krogh-Moe, *Acta Cryst.*, 1956, **9**, 951-953.

72   N. Norman, *Acta Cryst.*, 1957, **10**, 370-373.

73   A. K. Soper, *Mol. Phys.*, 2009, **107**, 1667-1684.

74   A. C. Hannon, W. S. Howells and A. K. Soper, *Inst. Phys. Conf. Ser.*, 1990, 193-211.

75   E. Lorch, *J. Phys. C*, 1969, **2**, 229.

76   A. C. Hannon, *Rutherford Appleton Laboratory Report, RAL-93-063*, 1993.

77   T. Takaishi, J. S. Jin, T. Uchino and T. Yoko, *J. Am. Ceram. Soc.*, 2000, **83**, 2543-2548.

78   E. R. Barney, A. C. Hannon, D. Holland, D. Winslow, B. Rijal, M. Affatigato and S. A. Feller, *J. Non-Cryst. Solids*, 2007, **353**, 1741-1747.

79   A. C. Hannon, J. M. Parker and B. Vessal, *J. Non-Cryst. Solids*, 1998, **232**, 51-58.

80   A. C. Hannon, J. M. Parker and B. Vessal, *J. Non-Cryst. Solids*, 1996, **196**, 187-192.

81   Y. Dimitriev, V. Mihailova and E. Gattef, *Phys. Chem. Glasses*, 1993, **34**, 114-116.

82   C. Dayanand, G. Bhikshamaiah and M. Salagram, *Mater. Lett.*, 1995, **23**, 309-315.

83   E. Ellis, D. W. Johnson, A. Breeze, P. M. Magee and P. G. Perkins, *Philos. Mag. B*, 1979, **40**, 125-137.

84   R. J. Gillespie and E. A. Robinson, *Angew. Chem. Int. Edit.*, 1996, **35**, 495-514.

85   R. J. Gillespie and I. Hargittai, *The VSEPR Model of Molecular Geometry*, Prentice Hall International, London, 1991.

86   R. Gillespie and R. Nyholm, *Quarterly Reviews, Chemical Society*, 1957, **11**, 339-380.

87   A. C. Wright, *Phys. Chem. Glasses Eur. J. Glass Sci. Technol. B*, 2008, **49**, 103-117.

88   N. Bansal and R. H. Doremus, Handbook of glass properties, Academic Press, Orlando, 1986, pp. 54-56.

89   O. V. Mazurin, M. V. Streltsina and T. P. Shvaiko-Shvaikovskaya, *Handbook of glass data. Part A, silica glass and binary silicate glasses*, Elsevier, Amsterdam, 1983.

90   S. Kohara, J. Akola, H. Morita, K. Suzuya, J. K. R. Weber, M. C. Wilding and C. J. Benmore, *Proc. Natl. Acad. Sci. USA*, 2011, **108**, 14780-14785.

91   S. Kohara, K. Suzuya, K. Takeuchi, C. K. Loong, M. Grimsditch, J. K. R. Weber, J. A. Tangeman and T. S. Key, *Science*, 2004, **303**, 1649-1652.

92   S. Sen, H. Maekawa and G. N. Papatheodorou, *J. Phys. Chem. B*, 2009, **113**, 15243-15248.

93   S. Sen and J. A. Tangeman, *Am. Min.*, 2008, **93**, 946–949.

94   C. Larson, J. Doerr, M. Affatigato, S. Feller, D. Holland and M. E. Smith, *J. Phys.: Condens. Mat.*, 2006, **18**, 11323-11331.

95   N. K. Nasikas, T. G. Edwards, S. Sen and G. N. Papatheodorou, *J. Phys. Chem. B*, 2012, **116**, 2696-2702.

96   C. Finbak, *Acta Chem. Scand.*, 1949, **3**, 1279-1292.

97   V. F. Sears, *Neut. News*, 1992, **3**, 26-37.

98   D. Waasmaier and A. Kirfel, *Acta Cryst. A*, 1995, **51**, 416-431.

99   D. A. Keen, *J. Appl. Cryst.*, 2001, **34**, 172-177.